

Magnetic anisotropies in ultrathin fcc Fe(001) films grown on Cu(001) substrates

J. F. Cochran, J. M. Rudd, M. From, and B. Heinrich

Physics Department, Simon Fraser University, Burnaby, British Columbia, Canada V5A 1S6

W. Bennett, W. Schwarzacher, and W. F. Egelhoff, Jr.

Surface Science Division, National Institutes of Standards and Technology, Gaithersburg, Maryland 20899

(Received 8 August 1991)

Ferromagnetic resonance absorption measurements at 36.3 GHz and at room temperature have been used to determine the g factor and anisotropy parameters for a series of bilayers composed of two 3-ML-thick fcc Fe (001) films separated by a variable thickness of fcc Cu(001). The resonance field and linewidth were measured versus the out-of-plane magnetic-field angle, θ_H . The magnetic properties of these ten coupled bilayer films were found to be remarkably similar from specimen to specimen, despite the fact that each member of the bilayer was only 3 ML thick. The average g factor was found to be $\langle g \rangle = 2.08 \pm 0.02$, and the average effective magnetization was found to be -5.5 ± 0.5 kOe; i.e., the specimens were magnetized normal to the specimen plane in zero applied magnetic field. If the effective field along the specimen normal can be attributed to a second-order surface anisotropy energy of the form $F_s = -K_{U1} \sin^2 \theta_M$, then $\langle K_{U1} \rangle = 1.25 \pm 0.06$ erg/cm², assuming a value $4\pi M_s = 21.6$ kOe for the saturation magnetization and using $d = 5.4$ Å for each film thickness. (This energy includes both sides of the film; the energy corresponding to a single Fe-Cu interface is 0.63 erg/cm².) These specimens exhibited no measurable in-plane anisotropy. The linewidth was found to exhibit a sharp decrease for θ_H near 20°. This decrease could be explained in terms of the angular dependence of inhomogeneous line broadening due to a 1% variation in the perpendicular effective field from place to place in the sample plane.

INTRODUCTION

We have used out-of-plane ferromagnetic resonance absorption measurements (FMR) at 36.3 GHz, and at room temperature, to determine the magnetic parameters for a series of fcc Fe(001) bilayers which were grown and used by Bennett, Schwartzacher, and Egelhoff¹ for magneto-optical Kerr effect studies. These bilayer structures were grown epitaxially on bulk fcc Cu(001) single-crystal substrates and consisted of two 3-monolayer-thick (3 ML) iron films separated by a layer of fcc Cu(001) of variable thickness. The iron bilayers were covered by 60 ML of fcc Cu(001) in order to protect them from oxidation when they were removed from the vacuum system. The thickness of the Cu spacer layer ranged from 3 to 30 ML. The Kerr effect measurements showed that the iron films were coupled by an interaction whose strength varied with the spacer layer thickness. The coupling strength was found to be an oscillatory function of thickness with peaks in the antiferromagnetic coupling at spacer thicknesses of approximately 8, 15, 22, and 30 ML.

Unfortunately, FMR absorption is not sensitive to the strength of interaction between two ultrathin films which have identical magnetic properties. The microwave magnetic field is essentially uniform in the plane of the specimen; it can therefore couple strongly only to modes in the film for which the deviation of the magnetization from equilibrium is uniform in the plane. The frequency spectrum for such modes is similar to the frequency spectrum for a single thin film, but each of the single-film mode fre-

quencies is split into a doublet because of the interaction between the two films. The frequency interval between the two members of a doublet is proportional to the strength of the interaction between the films. The lowest frequency doublet corresponds to modes in which all the spins within a given film precess in phase. Higher-frequency doublets correspond to a spatial variation of the magnetization across each film. Roughly speaking, this spatial variation corresponds to a wave number $k = n\pi/d$, where n is an integer and d is the film thickness.²

Any spatial variation of the magnetization within a film increases the energy of a mode, and hence increases the mode frequency, because of the exchange coupling between spins. For iron films 3 ML thick only the lowest-frequency doublet can be investigated using microwave frequencies. The next lowest-frequency doublet occurs at a mean frequency of approximately 22 000 GHz (corresponding to a free-space wavelength of 14 μ m) because of the very strong exchange torques which tend to keep the spins within a given film aligned. The lowest-frequency doublet corresponds to modes²⁻⁵ in which the spins within each film precess in phase but the spins in one film precess either in phase with the spins in the second film (acoustical mode) or in antiphase (optical mode). If the coupling between two identical films is ferromagnetic, the acoustical mode frequency is smaller than the optical mode frequency. For antiferromagnetic coupling between identical films the optical mode frequency is less than the acoustical mode frequency. A uniform microwave driving field cannot couple to the op-

tical mode for a pair of magnetically identical films because a uniform rf magnetic field having the same amplitude and phase within each film of the pair can exert no net torque on the system.

In our experiments, the thickness of each iron film ($\sim 5.4 \text{ \AA}$) as well as the spacing between the films ($\leq 54 \text{ \AA}$) were very small compared with the 36-GHz-microwave skin depth for bulk copper and iron at 300 K: $\delta = \sqrt{c^2/4\pi\omega\sigma} = 0.24 \text{ \mu m}$ for copper and $\delta = 0.59 \text{ \mu m}$ for iron. The rf magnetic field had, therefore, essentially the same amplitude and phase within each iron film. Only one absorption peak could be observed as the magnetic field was swept at fixed frequency, and that absorption peak corresponded to excitation of the acoustical mode.

The frequency of the acoustical mode is very insensitive to the strength of the interfilm coupling because all spins remain parallel as they precess in phase.³ The FMR spectrum for a coupled pair of identical films is the same as the spectrum for a single film, except for a doubling of the absorbed power, so long as the internal effective magnetic field remains large enough so that the system is always magnetically saturated. This condition was satisfied for the 36.3-GHz-FMR measurements reported below.

The angular dependence of the FMR field when the direction of the applied field is rotated in plane provides a direct measure of the in-plane components of the magnetocrystalline anisotropy terms in the magnetic free energy of the system. The angular dependence of the resonance field as the applied field is rotated out of the plane provides a direct measure of the g factor and the magnetic anisotropy terms associated with the direction along the specimen normal. The angular dependence of the FMR linewidth for fields directed out of plane provides information about the intrinsic magnetic damping in the films, and also provides information about inhomogeneous line broadening. All of the films which we investigated exhibited a striking increase in signal strength as the field was rotated out of the plane through an angle of $\sim 20^\circ$. This can be understood if much of the FMR absorption linewidth is caused by inhomogeneous line broadening as was suggested by Chappert *et al.*⁶ and by Purcell *et al.*⁷ Their idea is that the specimen can be regarded as a collection of independent regions; each region is supposed to be subject to a different anisotropy field in the direction normal to the plane and, therefore, to possess a different FMR resonant field. When the magnetic field is applied at $\sim 20^\circ$ from the plane (in the case of our iron films) the FMR field becomes very insensitive to the value of the anisotropy field so that all regions tend to absorb at the same value of applied magnetic field. It follows that the minimum linewidth provides a measure of the linewidth for a homogeneous iron film, and the increase in linewidth observed for the in-plane orientation provides a measure of the distribution of anisotropy fields. It will be demonstrated below that our observations are consistent with anisotropy distributions whose half-widths are less than 1% of their average value. The magnetic properties of these coupled bilayer films are remarkably similar from specimen to specimen despite the fact that each member of the bilayer is only 3 ML thick.

EXPERIMENTAL DETAILS

Fe(001) single-crystal specimens were grown on fcc Cu(001) single-crystal substrates in ultrahigh vacuum ($p \leq 10^{-10}$ Torr) by means of molecular beam epitaxy as described by Steigerwald, Jacob, and Egelhoff.⁸ Cu(001) crystal substrates were cut from a boule using a diamond saw. The resulting mechanical damage was removed from each side of a substrate by means of an acid facing instrument.⁹ The substrate was then polished to a mirrorlike finish using a solution of $\text{CuCl}_2 + \text{HCl} + 2\text{-mercaptobenzothiazole}$.¹⁰

Most of the substrates were, at this point, in the form of disks ~ 1 cm in diameter and between 1 and 2 mm thick. The substrates were subsequently cleaned in ultrahigh vacuum ($\sim 10^{-10}$ Torr) by ion sputter etching both sides for 2 h at room temperature, followed by several hours of sputtering at 1000 K. Following this initial cleaning cycle, the surface was cleaned by means of several minutes of sputtering at room temperature followed by a 30-s anneal to 700 K. This resulted in a surface which was clean within the XPS detection limit and which exhibited a sharp $p(1 \times 1)$ LEED pattern having a low background. The RHEED pattern exhibited sharp, elongated streaks, which indicated that the surface consisted predominantly of flat terraces.

Approximately 10 ML of Cu(001) were deposited at 450 K on the clean substrate surfaces. This homoepitaxial layer buried residual imperfections, thereby improving surface quality. The iron was deposited on a substrate cooled to 100 K and subsequently annealed at 350 K. These procedures are known to produce 3-ML-thick iron films in which the Fe-Cu interfaces are atomically smooth.⁸ The Cu(001) spacer layer was deposited at 350 K. The substrate was cooled to 100 K and the second iron layer was deposited and annealed at 350 K. A 60-ML-epitaxial Cu(001) coverlayer was deposited at 350 K; this overlayer protected the iron film from oxidation when the specimens were removed from the vacuum system in order to perform the magnetic measurements. It also ensured that each of the two iron films was surrounded by a similar fcc Cu(001) environment.

FMR measurements were carried out at room temperature using a microwave frequency of 36.3 GHz. The specimens formed part of the end wall of a cylindrical microwave cavity operated in the TE_{012} mode. A 0.005-in.-thick copper diaphragm was used to shield all but a central region of the specimen 5 mm in diameter from the microwave fields. Absorption was monitored by means of the signal reflected from the undercoupled cavity. The microwave frequency was locked to the resonant frequency of the cavity. Conventional field modulation at 176 Hz was used together with a lock-in amplifier to obtain a signal whose strength was proportional to the magnetic field derivative of the FMR absorption in the specimen. The cavity was mounted between the poles of a Varian 16-in. electromagnet; the field could be swept from 0 to 16.5 kOe. The magnet rotation axis was oriented perpendicular to the specimen normal so that the field could be rotated from a direction parallel with the specimen plane ($\theta_H = 0^\circ$, the parallel configuration) to a direction parallel

with the specimen normal ($\theta_H = 90^\circ$, the perpendicular configuration). The angular resolution was approximately 0.2° . Magnetic fields were calibrated against the NMR signal of protons in water.

In addition to the FMR measurements, Brillouin light scattering experiments (BLSS) were carried out on four of the specimens at room temperature using approximately 100 mW of 5145 \AA laser light incident at 45° to the film normal. The backscattered light was analyzed by means of a Sandercock 4+2 pass Fabry-Perot interferometer.¹¹ An external magnetic field, variable between 0 and 11 kOe, was applied in the plane of the film and perpendicular to the optical scattering plane. It is estimated from previous measurements¹² that the local temperature increase due to the focused laser light was less than 24°C . A free-spectral range of 30 GHz was used for most of the measurements. It is estimated that magnon frequencies could be determined within $\pm 0.5 \text{ GHz}$.

RESULTS

FMR data are shown for two specimens in Fig. 1 for applied fields oriented at 0° , 90° , and $\sim 20^\circ$ with respect to the sample plane. The iron films in these two specimens were separated by 3 ML and by 30 ML of Cu; these two spacer layer thicknesses represent the extremes of the range which were used for our experiments. The behav-

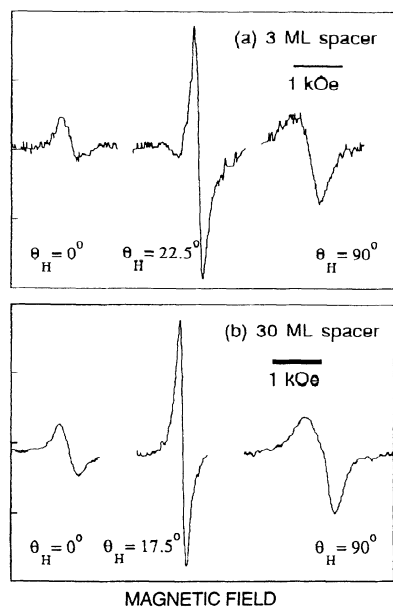


FIG. 1. FMR absorption derivative signals vs magnetic field measured using bilayer specimens composed of 3-ML-thick fcc Fe(001) films separated by Cu(001) spacer layers. Data for three out-of-plane magnetic field angles are shown: $\theta_H = 0^\circ$ (in plane), $\theta_H = 90^\circ$ (field applied along the specimen normal), and θ_H corresponding to the maximum derivative signal. (a) 3 ML spacer layer: ferromagnetic resonances occurred at 14.7, 12.7, and 8.5 kOe corresponding to 0° , 22.5° , and 90° . (b) 30 ML spacer layer: ferromagnetic resonances occurred at 16.2, 13.4, and 6.4 kOe corresponding to 0° , 17.5° , and 90° . The vertical gain corresponding to (a) was 4.9 times the vertical scale corresponding to (b). The heavy horizontal bar indicates a field interval of 1 kOe.

ior shown in Fig. 1 was typical for all of our samples. In particular, they all exhibited a dramatic increase in signal strength as the applied magnetic field was rotated out of the plane. This increase in absorption derivative amplitude was the consequence of a decrease in FMR linewidth. The minimum linewidth occurred for a rotation of the field through approximately 20° out of the plane; the minimum linewidth ranged from 100 to 200 Oe (see Fig. 3). The linewidth for the perpendicular configuration ($\theta_H = 90^\circ$) was usually found to be larger than the linewidth for the parallel configuration ($\theta_H = 0^\circ$) although the signal strength for the perpendicular orientation was always found to be stronger than the signal strength for the parallel configuration. This can be partially attributed to an increased active area for FMR absorption when the field was oriented perpendicular to the specimen plane. The rf magnetic field lines are radially directed for the cylindrical TE_{01} mode. In the parallel configuration the rf and static magnetic fields are nearly parallel over much of the specimen area and so these areas do not contribute strongly to the microwave absorption. On the other hand, in the perpendicular configuration the rf and static magnetic fields are perpendicular over the entire specimen area and as a result the entire exposed area contributes to the absorption. The field corresponding to maximum microwave absorption was taken to be the field midway between the fields corresponding to the absorption derivative extrema; it is estimated that this field value was uncertain to $\sim \pm 60 \text{ Oe}$ due to noise on the signals. Absorption linewidths were uncertain by a similar margin.

BLS experiments were carried out on the specimens having copper spacer layer thicknesses of 3, 12, 15, and 30 ML. The signals were generally weaker than signals measured¹³⁻¹⁵ using single 3-ML-thick fcc iron films grown on Cu(001), and the linewidths were quite broad. The best data were obtained using the specimen having a 30-ML-spacer layer, Fig. 2. The frequency increase for fields less than $\sim 6 \text{ kOe}$ occurs because the magnetization begins to turn out of the specimen plane at low magnetic fields; in zero applied field the magnetization is directed along the specimen normal.¹³⁻¹⁶ The linewidths were approximately 2 GHz for fields less than 7 kOe; they appeared to be approaching the instrumental resolution ($\sim 0.5 \text{ GHz}$) as the magnetic field was increased to 11 kOe. The 2-GHz spread in frequencies shown in Fig. 2 at an applied field of 7 kOe represents frequencies measured at different places on the specimen. The light used for the BLS measurements was focused to a spot approximately $20 \mu\text{m}$ in diameter so that it could be used as a kind of microprobe to examine the spatial variation of magnon frequencies. The magnon frequencies appeared to vary in an erratic manner from place to place on the sample—this provides direct evidence for spatial inhomogeneity of the magnetic properties of these films. All four specimens examined using BLS exhibited variations in magnon frequencies of the order of 2 GHz as the probe spot was removed from place to place on the sample. The sample containing a 15-ML-spacer layer exhibited particularly broad magnon lines for fields less than 8 kOe; they were $\sim 10 \text{ GHz}$ wide. It appeared that the magneti-

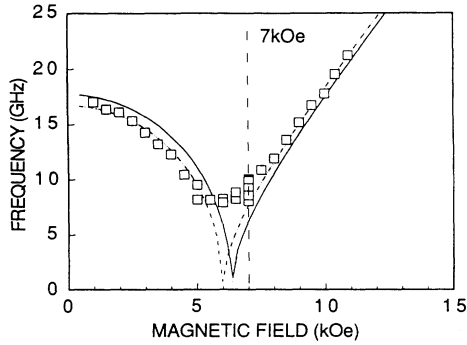


FIG. 2. Magnon frequency vs applied magnetic field for a magnetic bilayer composed of 3-ML-thick fcc Fe(001) films separated by a 30-ML-thick fcc Cu(001) spacer layer. The magnetic field was applied parallel with the specimen plane ($\theta_H = 0^\circ$). Magnon frequencies were measured with a precision of approximately 0.5 GHz by means of BLS using 5145 Å laser light incident at 45° in the backscattering configuration. Frequencies measured at different places on the specimen resulted in the ~ 2 GHz variation at 7 kOe shown in the figure: a variation of 2 GHz corresponds to a variation of 0.68 kOe in resonant magnetic field. The solid curve was calculated using the parameters listed in Table I obtained for this specimen using the FMR data. The dashed line was calculated using the same parameters except that $4\pi M_{\text{eff}} = -6.0$ kOe instead of the value -6.34 kOe required by the FMR data.

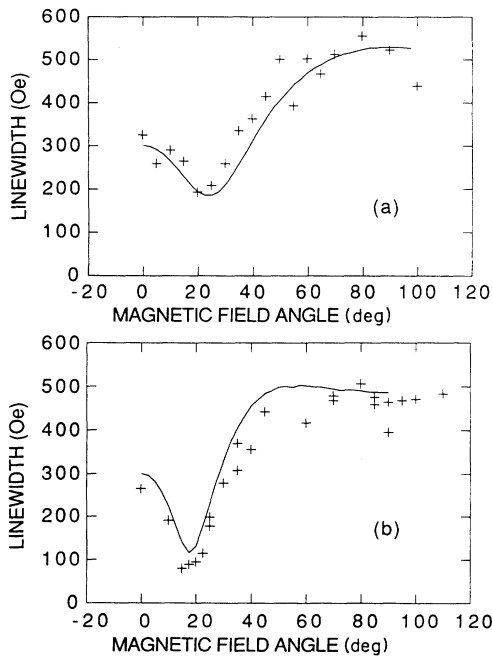


FIG. 3. Variation with magnetic field angle θ_H of the FMR linewidth measured for two 3-ML-thick fcc Fe(001) layers separated by an fcc Cu(001) spacer layer. $\theta_H = 0^\circ$ corresponds to a magnetic field applied in plane: (a) 3-ML spacer layer. (b) 30-ML spacer layer. The solid lines were calculated using the relevant parameters from Tables I and II.

zation in this sample was not fully saturated for in-plane magnetic fields less than ~ 8 kOe: the linewidth decreased dramatically as the applied field was increased to 10 kOe. This behavior would be consistent with the presence of relatively strong antiferromagnetic coupling between the two iron films as was deduced from the Kerr effect data.¹

The variation of FMR linewidth with the orientation of the applied magnetic field is shown in Fig. 3 for the bilayers having spacer thicknesses of 3 ML [Fig. (3a)] and 30 ML [Fig. (3b)]. All of the specimens which we measured exhibited qualitatively similar variations of linewidth versus applied magnetic field angle.

ANALYSIS

The results of the FMR absorption measurements will be compared with a model in which the average magnetization density M_s in a film of thickness d makes an angle of θ_M with respect to the film plane when an external uniform magnetic field is applied at an angle θ_H with respect to the film plane. It is assumed that \mathbf{H} and \mathbf{M}_s lie in the x - z plane, Fig. 4. It is further assumed that x, z lie along the cubic axes of the crystal. It is supposed that all the spins across the film precess in phase when they are disturbed from their equilibrium orientation. This hypothesis can be confirmed for a thin film by detailed calculations.¹⁷⁻¹⁹

The magnetic free-energy density of the system is taken to have the form

$$F = F_H + F_D + F_A + F_S, \quad (1)$$

where F_H is the contribution due to the applied magnetic field H ,

$$F_H = -HM_s \cos(\theta_H - \theta_M) \text{ erg/cm}^3; \quad (2)$$

the demagnetizing field energy is given by

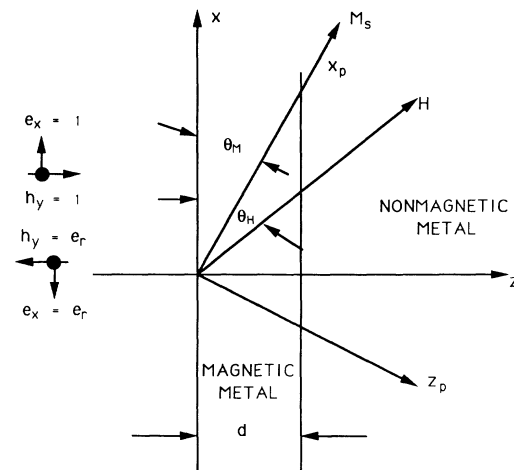


FIG. 4. Geometrical configuration used in the text to discuss the absorption of microwave radiation falling at normal incidence on the surface of a thin magnetic slab having a thickness d . The uniform magnetic field \mathbf{H} and the saturation magnetization density \mathbf{M}_s make angles of θ_H and θ_M with respect to the film plane.

$$F_D = 2\pi D_z M_s^2 \sin^2 \theta_M \text{ erg/cm}^3. \quad (3)$$

For a thick crystal the demagnetizing coefficient is given by $D_z = 1$. For an ultrathin crystal D_z is expected to be less than 1 (see Ref. 20). The contribution to the free energy per unit volume due to magnetocrystalline anisotropy can be written

$$F_A = -\frac{K_{1p}}{2} \left[\left(\frac{m_x}{M_s} \right)^4 + \left(\frac{m_y}{M_s} \right)^4 \right] - \frac{K_{11}}{2} \left[\left(\frac{m_z}{M_s} \right)^4 \right] - K_u \left(\frac{m_z}{M_s} \right)^2 \text{ erg/cm}^3. \quad (4)$$

The anisotropy terms in Eq. (4) may include both volume and surface contributions. In very thin magnetic films any surface energy terms which arise because of the broken symmetry at the surfaces become important.²¹ Our films are so thin that a torque exerted on a surface spin is transmitted to all of the interior spins by the very strong exchange interaction.¹⁷⁻¹⁹ A surface free-energy term of the form

$$F_{\text{surf}} = -K_{U1} \sin^2 \theta_M - K_{U2} \sin^4 \theta_M \text{ erg/cm}^2 \quad (5)$$

will therefore have the same effect as a volume free-energy contribution of the form

$$F_S = -\frac{K_{U1}}{d} \sin^2 \theta_M - \frac{K_{U2}}{d} \sin^4 \theta_M \text{ erg/cm}^3. \quad (6)$$

Volume and surface contributions to the anisotropy energy can be separated if measurements can be carried out for a range of film thicknesses. In the present case this separation into volume and surface contributions was not possible because data for only one thickness was available (3 ML = 5.4 Å). For the sake of definiteness, it was convenient to ascribe the perpendicular anisotropy entirely to either volume or surface terms; we have chosen to describe our results in terms of a surface free energy of the form (5).

Given a particular applied field direction θ_H , the equilibrium magnetization direction θ_M is determined from the requirement that the free-energy density be a minimum. Small oscillations around the equilibrium configuration can be calculated from the Landau-Lifshitz equations of motion:

$$-\frac{1}{\gamma} \frac{\partial \mathbf{m}}{\partial t} = (\mathbf{M} \times \mathbf{H}_{\text{eff}}) - \frac{G}{\gamma^2 M_s^2} \left[\mathbf{M} \times \frac{\partial \mathbf{m}}{\partial t} \right], \quad (7)$$

where

$$x_{yy} = \frac{m_y}{h_0} = \frac{[H_y - (i\omega/\gamma)(G/\gamma M_s)] M_s}{[H_y - (i\omega/\gamma)(G/\gamma M_s)][H_z - (i\omega/\gamma)(G/\gamma M_s)] - (\omega/\gamma)^2}, \quad (11)$$

where

$$H_y = H \cos(\theta_H - \theta_M) + \frac{2K_{1p}}{M_s} (\cos^4 \theta_M - 3 \sin^2 \theta_M \cos^2 \theta_M) + H_4 \sin^2 \theta_M (\sin^2 \theta_M - 3 \cos^2 \theta_M) + 4\pi M_{\text{eff}} (\cos^2 \theta_M - \sin^2 \theta_M) \quad (12)$$

$$\mathbf{M} = \mathbf{M}_s + \mathbf{m}, \quad (8)$$

$$(\mathbf{H}_{\text{eff}})_\alpha = -\frac{\partial F}{\partial m_\alpha} + h_\alpha(t), \quad (9)$$

and $\alpha = x, y$, or z . $\mathbf{h}(t)$ in (9) is a time-varying microwave magnetic field. The last term in (7) is a damping torque in the Gilbert form, and G is the Gilbert damping parameter whose units are per second (Hz). The magnetomechanical ratio is given by $\gamma = g|e|/2mc$; for $g = 2.000$ one has $\gamma = 1.7588 \times 10^7$ rad/Oe s.

For simplicity, consider a microwave plane wave having its magnetic vector polarized along y falling at normal incidence on the specimen (Fig. 4). It is assumed that the ferromagnetic thin film is mounted on a thick conducting substrate. A microwave plane wave incident on a conducting surface will be reflected with an amplitude which is very nearly equal to the amplitude of the incident wave, but its electric vector will be reversed so that the total electric field amplitude at the metal surface will be very nearly equal to zero. The magnetic field components in the incident and reflected waves add in phase so that the rf magnetic field amplitude at the surface is just twice the amplitude in the incident wave. Furthermore, if the magnetic film thickness is very small compared with the microwave skin depth, δ , then the rf magnetic field in the film will be nearly uniform and equal to twice the amplitude in the incident wave. This conclusion has been checked by solution of Maxwell's equations using the appropriate boundary conditions and the bulk conductivities for copper and iron. The skin depth in bulk iron at 300 K and for a frequency of 36 GHz is given by $\delta = \sqrt{c^2/4\pi\omega\sigma} = 0.59 \mu\text{m}$. At FMR the skin depth is reduced approximately by a factor of 10. In our experiments each iron film was only 5.4 Å thick, and the two films were separated by 60 Å of copper at most. It is therefore very reasonable to use a model in which the magnetizations in the two films are driven by the same microwave field.

The magnetic response of a thin magnetic film driven by a uniform magnetic field of the form

$$h_y = h_0 \exp(-i\omega t) \quad (10)$$

can be obtained from the Landau-Lifshitz equations (7). The calculation is most conveniently carried out in the rotated coordinate system x_p, y, z_p , of Fig. 4. This is a natural system for describing the motion of the magnetization since in equilibrium the magnetization lies along one of the axes. Using the free-energy expressions (4) and (6), the result of the calculation is

and

$$H_z = H \cos(\theta_H - \theta_M) + \frac{2K_{1p}}{M_s} \cos^4 \theta_M - 4\pi M_{\text{eff}} \sin^2 \theta_M + H_4 \sin^4 \theta_M. \quad (13)$$

In Eqs. (12) and (13) we have introduced the definitions

$$4\pi M_{\text{eff}} = 4\pi D_z M_s - \frac{2K_u}{M_s} - \frac{2K_{U1}}{dM_s}, \quad (14)$$

$$H_4 = \frac{2K_{11}}{M_s} + \frac{4K_{U2}}{dM_s}. \quad (15)$$

It can be shown from Maxwell's equations²² that the average rate at which energy is absorbed per unit area from the microwave driving field by the magnetic film is given by

$$\left\langle \frac{dU}{dt} \right\rangle = \left\langle d \left[h_y \frac{\partial m_y}{\partial t} \right] \right\rangle = \frac{\omega h_0^2 d}{2} \text{Im}(\chi_{yy}). \quad (16)$$

The absorption coefficient for the film can be written

$$\alpha = 16\pi d(\omega/c) \text{Im}(\chi_{yy}), \quad (17)$$

since the average rate at which microwave energy is carried to the specimen surface is $\langle S_z \rangle = (ch_0^2/32\pi)$ per cm^2 ; remember that h_0 is the rf magnetic field amplitude inside the magnetic film and therefore the incident magnetic field amplitude is $h_0/2$. According to this theory, the absorption at fixed frequency in the parallel and perpendicular configurations is very nearly a Lorentzian whose linewidth is approximately $(\omega/\gamma)(G/\gamma M_s)$ Oe. However, when the external static field is applied at some intermediate angle the angle between the magnetization direction and the plane, θ_M , varies with the applied field strength.²³ This dragging effect causes the absorption linewidth to become somewhat larger than that corre-

sponding to $\theta_H = 0$. We have written a computer program with which the variation of absorption with field strength at fixed frequency can be calculated taking into account the change of magnetization angle with field strength. The output of the program gives the field corresponding to maximum absorption, H_r , and the field interval between absorption derivative extrema, i.e., the linewidth ΔH . Measured resonant fields were compared with calculated resonant fields for approximately 20 angles uniformly spread between the parallel configuration, $\theta_H = 0^\circ$, and the perpendicular configuration, $\theta_H = 90^\circ$. The effective magnetization, Eq. (14), the fourth-order effective field, H_4 , Eq. (15), the g factor, and the magnet error angle, $\delta\theta_H$, were varied to produce the best least-squares fit between the observed and calculated resonant fields. The parameter $\delta\theta_H$ was included because it was difficult to determine to better than 1° - 2° the magnet angle setting which corresponded to an in-plane magnetic field orientation. The damping parameter G was not used as a fitting parameter because the resonant field H_r is very insensitive to G ; we used the value determined from the absorption linewidth (see below). The volume anisotropy parameter K_{1p} was set equal to zero because the FMR field was found to be independent of field orientation in the specimen plane within the experimental uncertainty of ~ 100 Oe. The results obtained from these fits are listed in Table I along with the root-mean-square values for the residuals. The quality of the fits obtained was excellent; in most cases the difference between calculated and observed resonant fields was less than 50 Oe. The worst fit was obtained for the 30-ML-Cu spacer layer; see Fig. 5.

TABLE I. Parameters used to describe the variation with out-of-plane angle of the FMR resonant magnetic field measured at 36.3 GHz and at room temperature. $4\pi M_{\text{eff}} = 4\pi D_z M_s - 2K_{U1}/dM_s$ and $H_4 = 4K_{U2}/dM_s$ [see Eqs. (12) and (13) of the text and following. It is assumed that the anisotropies are due to surface terms]. Negative $4\pi M_{\text{eff}}$ means that the magnetization will be oriented perpendicular to the specimen plane in zero applied magnetic field.

Cu spacer layer thickness d (ML)	g	$-4\pi M_{\text{eff}}$ (kOe)	$-H_4$ (kOe)	Root-mean-square residual (Oe)	Second-order surf. param. ^a K_{U1} (erg/cm ²)	Fourth-order surf. param. ^a K_{U2} (10^{-3} erg/cm ²)
3	2.091	4.17	0.28	35	1.19	-6.6
9	2.083	5.34	0.048	20	1.25	-1.1
12	2.077	6.04	0.054	28	1.28	-1.2
14	2.082	4.76	0.064	35	1.22	-1.5
15 ^b	2.096	5.89	0.37	30	1.27	-8.5
15 ^b	2.062	6.09	0.34	37	1.28	-7.9
16	2.072	5.45	0	28	1.25	0
17	2.070	5.33	0.015	22	1.25	-3.5
19	2.081	5.10	0.093	21	1.23	-2.2
22	2.102	6.15	0.10	16	1.28	-2.3
30	2.068	6.34	0.21	51	1.29	-4.8

^aUsing $4\pi M_s = 21.55$ kOe, $D_x = 1$, and $d = 5.4$ Å.

^bIndependent measurements using the same 15-ML-spacer layer specimen.

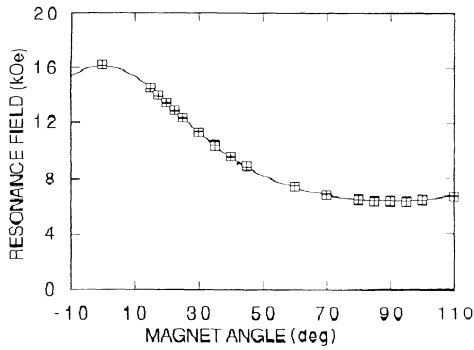


FIG. 5. FMR resonance field vs out-of-plane magnetic field angle for a magnetic bilayer composed of two 3 ML fcc Fe(001) films separated by 30 ML of fcc Cu(001). The solid curve was calculated using the parameters from Table I and $G=2.16 \times 10^8$ Hz.

ABSORPTION LINEWIDTH

According to the simple theory described in the previous section, the FMR linewidth should increase slightly as the magnetic field is rotated out of the specimen plane. It should reach a maximum for angles θ_H between 40° and 50° and then decrease so that the linewidths become the same for the parallel and perpendicular configurations. This behavior is shown in Fig. 7, curve (a), where the angular dependence of the linewidth has been calculated using $G=3.78 \times 10^8$ Hz and the other parameters for the 3-ML-spacer layer specimen, Table I. A comparison between Fig. 7, curve (a) and the linewidth data for this specimen shown in Fig. (3a) clearly shows that the data cannot be described by the simple theory using an angularly independent damping parameter.

The damping parameter measured for bulk metals at room temperature to date has been found to be independent of orientation. The BLS data suggest that the specimen is composed of many regions having slightly different magnetic properties. We have therefore analyzed our linewidth data using the model of inhomogeneous line broadening suggested by Purcell *et al.*⁷ (It is interesting to note that a similar model was used by Rossing²⁴ to discuss linewidth broadening in thin Permalloy films.) According to this model the specimen is composed of a large number of independent absorbers all having the same g factor and intrinsic magnetization but having different anisotropy parameters. We have no data on the thickness dependence of the anisotropies but, for the sake of simplicity, we have assumed that in these films they are entirely due to surface effects; this seems very plausible since most of the atoms in the film are sited at a surface. Thus in the expression for the effective magnetization, Eq. (14), the term proportional to K_u has been set equal to zero. Similarly, in the expression for the fourth-order anisotropy field, H_4 [see Eq. (15)], the term proportional to K_{11} has been set equal to zero. The linewidth inhomogeneous broadening is assumed to be due to a distribution in the two surface anisotropy parameters K_{U1} and K_{U2} [see Eq. (6)].

The surface energy parameter K_{U1} is assumed to be

distributed around its mean value $\langle K_{U1} \rangle$ according to a Gaussian distribution:

$$P(K_{U1}) \propto \exp \left[-\frac{1}{2} \left(\frac{K_{U1} - \langle K_{U1} \rangle}{\sigma_K} \right)^2 \right]. \quad (18)$$

We needed an extra degree of freedom in order to fit the linewidth data both for parallel and perpendicular magnetic fields as well as at the angle corresponding to minimum linewidth. We therefore have assumed that variations in the second-order anisotropy parameter, K_{U1} , are accompanied by variations in the fourth-order anisotropy constant, K_{U2} . Thickness variations could provide one plausible source for such a coupling between variations in these two parameters since both terms in the free-energy expression for F_s are inversely proportional to thickness, Eq. (6). We have used the relation

$$K_{U2} = \langle K_{U2} \rangle + X_B (K_{U1} - \langle K_{U1} \rangle). \quad (19)$$

A normalized Gaussian probability distribution was used to calculate the magnetic field dependence of the absorption in an inhomogeneous specimen having due regard for the dependence of the magnetization angle θ_M on field in each subregion. The introduction of the distribution (18) has the effect of broadening the absorption line at all angles θ_H , but the maximum broadening occurs at 0° and at 90° . The dramatic decrease in linewidth which is predicted to occur for angles near 20° , in agreement with experiment, can be understood with reference to Fig. 6. In Fig. 6 the FMR resonance field has been calculated for three different values of the surface energy parameter K_{U1} : a value corresponding to the mean deduced from the resonance field data for the 3-ML-spacer specimen, $K_{U1}=1.19$ erg/cm², see Table I, and values which are 10% larger and smaller than this mean value. It is obvious from Fig. 6 that the resonant field value becomes relatively insensitive to variations in K_{U1} for angles near 22° ;

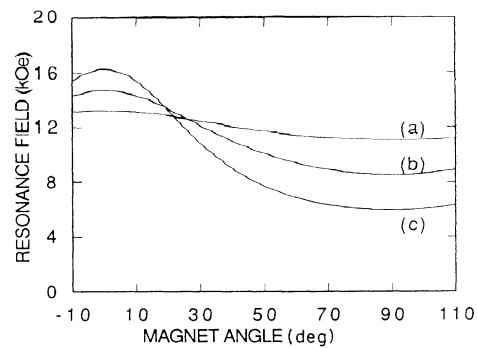


FIG. 6. Calculated variation of the FMR resonance field vs out-of-plane magnetic field angle for a 3-ML-thick film having the uniform magnetic properties listed in Table I for a 3-ML-spacer layer but for three values of the second-order surface energy parameter, K_{U1} . (a) $K_{U1}=1.07$ erg/cm². (b) $K_{U1}=1.19$ erg/cm². (c) $K_{U1}=1.31$ erg/cm². This figure illustrates the insensitivity of the resonant field to a distribution of K_{U1} values when the magnetic field is applied at an angle of $\sim 22^\circ$ to the film plane.

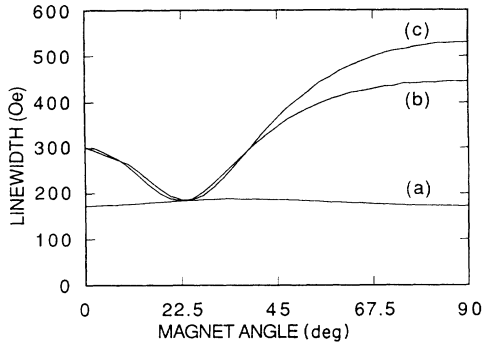


FIG. 7. Calculated variation of the FMR linewidth vs out-of-plane magnetic field angle for a 3-ML-thick magnetic film having the properties listed in Tables I and II for a 3-ML-thick spacer layer. (a) No variation in the anisotropy parameters; $\sigma_K=0$ and $X_B=0$. (b) A Gaussian distribution of the second-order surface energy parameter, K_{U1} , but no variation in the fourth-order anisotropy parameter, K_{U2} [see Eq. (6)]; $\sigma_K=7.75 \times 10^{-3}$ but $X_B=0$. (c) A Gaussian distribution of both the second-order surface anisotropy parameter K_{U1} and of the fourth-order surface energy parameter K_{U2} ; $\sigma_K=7.75 \times 10^{-3}$ and $X_B=0.124$.

thus the minimum inhomogeneous line broadening must occur near that angle. It is further clear from Fig. 6 that the linewidth at 90° should be larger than the linewidth at 0° in the absence of any contribution from variations in K_{U2} . In fact, the term in K_{U2} does not affect the field at which resonance occurs when $\theta_H=0^\circ$; the maximum effect occurs for $\theta_H=90^\circ$. Therefore variations in this parameter can be used to adjust the 90° linewidth without affecting the 0° linewidth. The calculated variation of linewidth with field angle is shown in Fig. 7 for parameters appropriate for the specimen containing a 3-ML-Cu spacer layer. It can be seen from this figure that the minimum linewidth is essentially equal to the linewidth expected for a homogeneous specimen. We have used the observed linewidths at 0° , at 90° , and at the angle corre-

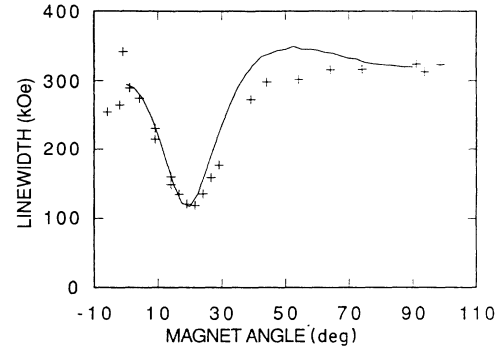


FIG. 8. FMR linewidth vs out-of-plane magnetic field angle for two 3-ML-thick fcc Fe(001) films separated by 14 ML of fcc Cu(001). The solid curve was calculated using the procedure described in the text and using the relevant parameters listed in Tables I and II. For this specimen, and for the specimens containing spacer layers 9 and 16 ML thick, the calculated linewidths tend to be larger than the measured linewidths for angles around 50° .

sponding to the minimum linewidth to determine the three fitting parameters G , σ_K , and X_B . These three parameters are not completely independent and therefore it was necessary to use an iterative procedure to determine them. The results are listed in Table II. These parameters were found to provide a satisfactory description for seven of the ten specimens which we investigated: the calculated curves shown in Fig. 3 are typical for this group. The linewidth curves calculated using the parameters listed in Table II for spacer thicknesses of 9, 14, and 16 ML are in less satisfactory agreement with the observations; see Fig. 8: the calculated linewidths are somewhat too large for angles near 45° . Apparently the simple model which assumes a direct proportionality between fluctuations in K_{U1} and K_{U2} does not work well for these three specimens. There is no other obvious way in which these three specimens differed from the majority of the bilayer specimens.

TABLE II. Parameters used to describe the variation with out-of-plane magnetic field angle of the FMR linewidth measured at 36.3 GHz and at room temperature. See Eqs. (18) and (19).

Cu spacer layer thickness d (ML)	Gilbert damping parameter G (10^8 Hz)	Half-width distribution $4\pi M_{\text{eff}}$ (kOe)	Half-width distribution K_{U1}, σ_K (10^{-3} erg/cm 2)	X_B
3	3.78	0.17	7.75	0.12
9 ^a	2.68	0.10	4.77	-0.24
12	2.71	0.18	8.24	0.03
14 ^a	2.34	0.23	8.77	-0.17
15 ^b	3.00	0.28	12.9	-0.17
15 ^b	3.29	0.18	8.13	0.02
16 ^a	2.20	0.30	13.7	-0.25
17	3.24	0.18	8.44	-0.15
19	3.64	0.16	7.25	-0.11
22	2.76	0.24	11.0	0.25
30	2.16	0.19	8.73	0.06

^aLess satisfactory fit to the linewidth data. See Fig. 8.

^bIndependent measurements using the same 15-ML-spacer layer specimen.

DISCUSSION

The results of measurements on ten bilayer specimens demonstrate that single-crystal fcc Fe(001) films grown on copper can be prepared with reproducible properties even though each film is only 3 ML thick. The data also demonstrate the relative ease with which FMR absorption methods can be used to obtain g factors and anisotropy parameters for ultrathin magnetic films. The utility of the FMR technique is based upon its good sensitivity and the high precision with which frequency and resonant magnetic fields can be routinely measured.

The g factor for 3-ML-thick fcc Fe(001) films was found to be $g = 2.08 \pm 0.02$. This value is very similar to that measured for bulk iron²⁵ and for ultrathin bcc iron films,^{26,27} i.e., $g = 2.09$. Polarized neutron reflection experiments²⁸ have shown that the magnetization density in 3-ML-thick fcc Fe(001) films, $4\pi M_s = 19.0 \pm 6$ kOe, is similar to the magnetization density for bulk bcc iron, $4\pi M_s = 21.6$ kOe. It appears that the basic magnetic properties of fcc and bcc iron are not very different.

These fcc iron films are found to be characterized by an out-of-plane magnetic anisotropy which is sufficiently large to cause the magnetization to be oriented perpendicular to the specimen plane in zero applied magnetic field. The effective field corresponding to this anisotropy is ~ 27 kOe since $4\pi M_{\text{eff}} \sim -5$ kOe [see Eq. (14)]. Assuming that this effective field can be ascribed to surface energy terms of the form given in Eq. (5), the principal term, the second-order term in which the energy is a quadratic function of the normal magnetization component, corresponds to a surface energy $K_{U1} = 1.25$ erg/cm² when averaged over all samples. This is the surface energy contributed by both surfaces of the film. The surface energy for a single fcc iron-copper interface would be 0.63 erg/cm², which is very comparable to that measured for the iron-silver interface^{27,29} using a 10-ML-thick film (0.81 erg/cm²), and measured for the iron-gold interface^{27,29} using a 10-ML-thick film (0.47 erg/cm²).

A discrepancy of approximately 1/2 kOe was found between values of the effective magnetization required to fit the BLS data and values of the effective magnetization deduced from the angular dependence of the FMR resonance field at 36 GHz. This is illustrated for the specimen having a 30-ML-Cu spacer layer in Fig. 2. From this figure it can be seen that the BLS data are more consistent with a value $4\pi M_{\text{eff}} = -6.0$ kOe than with the value $4\pi M_{\text{eff}} = -6.34$ kOe deduced from the FMR data. The reason for this discrepancy is not known. It may indicate that the anisotropy energies are slightly field dependent. The maximum parallel field used for the BLS measurements was 11 kOe; this can be compared with the FMR resonant field value of 15 kOe observed for the parallel configuration. The discrepancy cannot be due to an increase of saturation magnetization with increasing applied magnetic field due to an angular spread of magnetization directions in the plane: any increase in $4\pi M_s$ would cause the value of $4\pi M_{\text{eff}}$ to increase, i.e., to become less negative rather than more negative with increasing field as is observed.

A small fourth-order anisotropy term, which we have

arbitrarily ascribed to a surface term specified by the parameter K_{U2} [see Eq. (5)], was required to properly fit the FMR resonance field data: its value averaged over all specimens was found to be $K_{U2} = -3.6 \times 10^{-3}$ erg/cm². When the magnetization was oriented along the specimen normal this term created an effective field, $H_4 = 4K_{U2}/dM_s$, whose magnitude was found to be 0.16 kOe when averaged over all samples; its direction was opposed to the second-order anisotropy field H_U . The magnitude of K_{U2} was found to fluctuate from specimen to specimen around the mean by an amount comparable with the mean value. Moreover, the distribution in K_{U2} values within a given specimen required to explain the excess FMR linewidth observed when the applied field was oriented perpendicular to the specimen plane was comparable with the mean value of K_{U2} . If this fourth-order term has any physical significance at all it must be very sensitive to specimen morphology.

The FMR linewidth in ultrathin fcc Fe (001) films was found to be dominated by inhomogeneous line broadening when the field was applied along one of the "natural" orientations i.e., when applied either along the film normal or applied parallel to the thin-film plane. The linewidth measured for ultrathin Co films grown on Pd was also found to be dominated by inhomogeneous line broadening for fields applied in plane or along the specimen normal;⁷ the linewidth in these films decreased from ~ 0.88 kOe for an in-plane applied field to a minimum of ~ 0.44 kOe for fields applied at an angle of $\sim 35^\circ$ to the plane. This phenomenon is likely to be encountered whenever a film is subject to an anisotropy which tends to rotate the magnetization out of the plane. It follows that in such cases out-of-plane FMR linewidth measurements should be carried out in order to determine the linewidth for an equivalent homogeneous specimen. The damping parameters G , corresponding to an equivalent homogeneous specimen which were determined for the present films, were found to range from $(2.2-3.8) \times 10^8$ Hz. These figures can be compared with the values $G = 5.7 \times 10^8$ Hz measured²⁶ for 3-ML-thick bcc Fe films grown on Ag and $G = 1.8 \times 10^8$ Hz for 9.5-ML-thick bcc Fe films³⁰ grown on Ag. The damping parameter measured for room-temperature bulk bcc iron³¹ is $G = 0.7 \times 10^8$ Hz. Very likely much of the damping in these ultrathin iron films was caused by the relaxation of the magnetization due to two magnon processes³² facilitated by surface roughness; the surfaces undoubtedly contained many atomic steps. In principle, the contributions to the damping due to intrinsic processes such as spin-orbit coupling could be separated from two-magnon processes by measuring the frequency dependence of the equivalent homogeneous linewidth.^{26,30} The slope of linewidth versus frequency would be proportional to the intrinsic damping contribution, and the zero-frequency intercept would provide a measure of the contribution due to surface roughness and other physical defects in the films.³³

A variation of $\sim \pm 1\%$ in the perpendicular effective field due to anisotropy is all that is required to explain the observed inhomogeneous line broadening in our iron bilayers. If this anisotropy is ascribed to a surface energy term, then the effective field which enters the torque

equations, $H_U = 2K_{U1}/dM_s$, is inversely proportional to the film thickness. The relatively small variation of H_U from place to place in these samples indicates that the average thickness is very uniform.

ACKNOWLEDGMENT

The authors would like to thank the Natural Sciences and Engineering Research Council of Canada for grants that supported this work.

- ¹W. R. Bennett, W. Schwarzacher, and W. F. Egelhoff, Jr., *Phys. Rev. Lett.* **65**, 3169 (1990).
- ²P. Grünberg, *J. Appl. Phys.* **57**, 3673 (1985).
- ³B. Heinrich, S. T. Purcell, J. R. Dutcher, K. B. Urquhart, J. F. Cochran, and A. S. Arrott, *Phys. Rev. B* **38**, 12 879 (1988).
- ⁴B. Heinrich, Z. Celinski, J. F. Cochran, W. B. Muir, J. Rudd, Q. M. Zhong, A. S. Arrott, K. Myrtle, and J. Kirschner, *Phys. Rev. Lett.* **64**, 673 (1990).
- ⁵Z. Celinski, B. Heinrich, J. F. Cochran, W. B. Muir, A. S. Arrott, and J. Kirschner, *Phys. Rev. Lett.* **65**, 1156 (1990).
- ⁶C. Chappert, K. Le Dang, P. Beauvillain, H. Hurdequint, and D. Renard, *Phys. Rev. B* **34**, 3192 (1986).
- ⁷S. T. Purcell, H. W. Van Kesteren, E. C. Cosman, W. B. Zeper, and W. Hoving, *J. Appl. Phys.* **69**, 5640 (1991).
- ⁸D. A. Steigerwald, I. Jacob, and W. F. Egelhoff, Jr., *Surf. Sci.* **202**, 472 (1988); D. A. Steigerwald and W. F. Egelhoff, Jr., *Phys. Rev. Lett.* **60**, 2558 (1988).
- ⁹F. W. Young and T. R. Wilson, *Rev. Sci. Instrum.* **32**, 559 (1961).
- ¹⁰J. S. Ahearn, J. P. Monaghan, Jr., and J. W. Mitchell, *Rev. Sci. Instrum.* **41**, 1853 (1970).
- ¹¹J. R. Sandercock, in *Light Scattering in Solids III*, edited by M. Cardona and G. Güntherodt, Vol. 51 of *Topics in Applied Physics* (Springer, Berlin, 1982), Chap. 6.
- ¹²J. R. Dutcher, J. F. Cochran, B. Heinrich, and A. S. Arrott, *J. Appl. Phys.* **64**, 6095 (1988).
- ¹³J. R. Dutcher, B. Heinrich, J. F. Cochran, D. A. Steigerwald, and W. F. Egelhoff, Jr., *J. Appl. Phys.* **63**, 3464 (1988).
- ¹⁴J. R. Dutcher, J. F. Cochran, I. Jacob, and W. F. Egelhoff, Jr., *Phys. Rev. B* **39**, 10 430 (1989).
- ¹⁵J. F. Cochran, W. B. Muir, J. M. Rudd, B. Heinrich, Z. Celinski, and Tan-Trung Le-Tran, *J. Appl. Phys.* **69**, 5206 (1991).
- ¹⁶D. P. Pappas, K.-P. Kamper, B. P. Miller, H. Hopster, D. E. Fowler, A. C. Luntz, C. R. Brundle, and Z.-X. Shen, *J. Appl. Phys.* **69**, 5209 (1991).
- ¹⁷G. T. Rado, *Phys. Rev. B* **26**, 295 (1982); G. T. Rado and Lu Zhang, *ibid.* **33**, 5080 (1986).
- ¹⁸U. Gradmann, J. Korecki, and G. Waller, *Appl. Phys. A* **39**, 101 (1986).
- ¹⁹R. P. Erickson and D. L. Mills, *Phys. Rev. B* **43**, 10 715 (1991).
- ²⁰For a magnetic field oriented along the normal of a slab whose surfaces are (001) planes of an fcc crystal the demagnetizing factor can be written $D_z = (1 - 0.2338/N)$, where N is the number of monolayers. See B. Heinrich, M. Kowalewski, J. F. Cochran, J. Kirschner, Z. Celinski, A. S. Arrott, and K. Myrtle, *Phys. Rev. B* **44**, 9348 (1991). The demagnetizing factor for thin bcc films is discussed in the Appendix of Heinrich *et al.* (Ref. 3).
- ²¹L. Néel, *J. Phys. Radium* **15**, 225 (1954).
- ²²L. D. Landau and E. M. Lifshitz, *The Electrodynamics of Continuous Media* (Pergamon, New York, 1960), Sec. 61.
- ²³At each angle the magnitude of the applied field was much larger than the effective field associated with the exchange coupling between the two films in a bilayer: this effective field was at most 2 kOe for the specimens (Ref. 1) listed in Table I. We have, therefore, assumed that the static magnetization vectors in the two films remain parallel for all orientations of the applied field.
- ²⁴T. D. Rossing, *J. Appl. Phys.* **34**, 995 (1963).
- ²⁵Z. Frait and R. Gemperle, *J. Phys. (Paris) Colloq.* **32**, C1-541 (1971).
- ²⁶B. Heinrich, K. B. Urquhart, A. S. Arrott, J. F. Cochran, K. Myrtle, and S. T. Purcell, *Phys. Rev. Lett.* **59**, 1756 (1987).
- ²⁷B. Heinrich, J. F. Cochran, A. S. Arrott, S. T. Purcell, K. B. Urquhart, J. R. Dutcher, and W. F. Egelhoff, Jr., *Appl. Phys. A* **49**, 473 (1989).
- ²⁸W. Schwarzacher, W. Allison, R. F. Willis, J. Penfold, R. C. Ward, I. Jacob, and W. F. Egelhoff, Jr., *Solid State Commun.* **71**, 563 (1989).
- ²⁹B. Heinrich, Z. Celinski, J. F. Cochran, A. S. Arrott, and K. Myrtle, *J. Appl. Phys.* **70**, 5769 (1991).
- ³⁰Z. Celinski and B. Heinrich, *J. Appl. Phys.* **70**, 5935 (1991).
- ³¹J. M. Rudd, J. F. Cochran, K. B. Urquhart, K. Myrtle, and B. Heinrich, *J. Appl. Phys.* **63**, 3811 (1988).
- ³²M. Sparks, *Ferromagnetic Relaxation Theory* (McGraw-Hill, New York, 1964).
- ³³J. F. Cochran, K. Myrtle, and B. Heinrich, *J. Appl. Phys.* **53**, 2261 (1982); B. Heinrich, J. F. Cochran, and R. Hasegawa, *ibid.* **57**, 3690 (1985).